International Journal of Fluid Power 6 (2005) No. 2 pp. 47-56

MODELLING AND SIMULATION OF A HYDRAULIC BREAKER

Antonio Giuffrida and Domenico Laforgia

University of Lecce – Department of Engineering for Innovation, Via per Arnesano, 73100 Lecce, Italy
antonio.giuffrida@.unile.it, domenico.laforgia@unile.it

Abstract

This paper deals with the simulation of the working behaviour of a hydraulic breaker. A detailed parameterised model was realized in order to simulate physical phenomena occurring during the functioning of the machine. An appreciable agreement between experimental and theoretical pressure and frequency encouraged about the quality of the model. The dynamic behaviour of the moving masses was presented and thoroughly discussed. As a special remark, it is to be highlighted that the theoretical results suggested by the model came out not to vary if the real waveform concerning input flow rate is replaced with its average.

Keywords: hydraulic breaker, working cycle, mathematical model, simulation

1 Introduction

1.1 Background

The hydraulic breaker represents an indispensable equipment for demolition, construction, civil engineering, and even recycling works. Due to its versatile structure for various applications, the hydraulic breaker is one of the several tools used in an excavator and it should be correctly chosen in order to achieve the performance warranted by the manufacturer. It consists of a machine turning the hydraulic energy supplied by a positive displacement pump into mechanical energy in terms of percussions against a chisel. The latter is appointed to crumble a certain material by means of alternating impacts.

The bibliographic research carried out by the authors showed that literature seems to lack in technical papers dealing with such typology of hydraulic machines. So that only two papers were found in the international literature. In the first one (Gorodilov, 2000), an approach to the analysis of the working cycle of the breaker by means of similarity criteria is presented. Referring to a simple schematisation of the machine, a system of equations governs its functioning even if an ideal behaviour of the distributor, managing the dynamics of the striking mass inside the breaker, was hypothesized. The physical meaning of the similarity criteria is obvious since most of them reflect the geometric features of the breaker and the magnitudes of mechanical and hydraulic parameters. In (Gorodilov, 2002), there are shown different shapes of piston movements and velocities and pressure evolutions as well. These shapes are properly dimensionless on the basis of the previously introduced and further simplified formulations. Equations and results presented in these works are undoubtedly relevant since they allow a preliminary selection of the basic parameters of hydraulic percussive machines. However, they only concern themselves with a theoretical analysis of a machine whose distributor is idealized as an on-off valve switching from two fixed positions. Thus, these works do not set forth a general model that would result more useful for better looking into the functioning of the breaker.

This manuscript was received on 17 December 2004 and was accepted after revision for publication on 12 June 2005

1.2 Breaker working principle

The functioning of a hydraulic breaker is presented with reference to (European Patent no. 0085279; European Patent no. 0426928) and to the schematic drawing shown in Fig. 1.

The reciprocating motion of the piston (PIS) striking the chisel (CH) is obtained thanks to a distributor (DIS) which alternatively places the downward push chamber (V1) in communication with a high pressure circuit, to give it impact power, and with a low pressure circuit, to bring the piston back to its top dead center whose position is usually variable depending on the material to crumble. The movement towards this posi-

tion is caused by the force always exerted by the high pressure oil on the piston small ring area at the upward push chamber (V2), opposite to the wider circular area at the top of the piston. The distributor consists of a cylindrical sleeve valve connected to a flange-type ring plate at its bottom. It can move in a ring chamber (V3) realized in the casing. The upward movement of the distributor is caused by high pressure fluid acting on different areas.

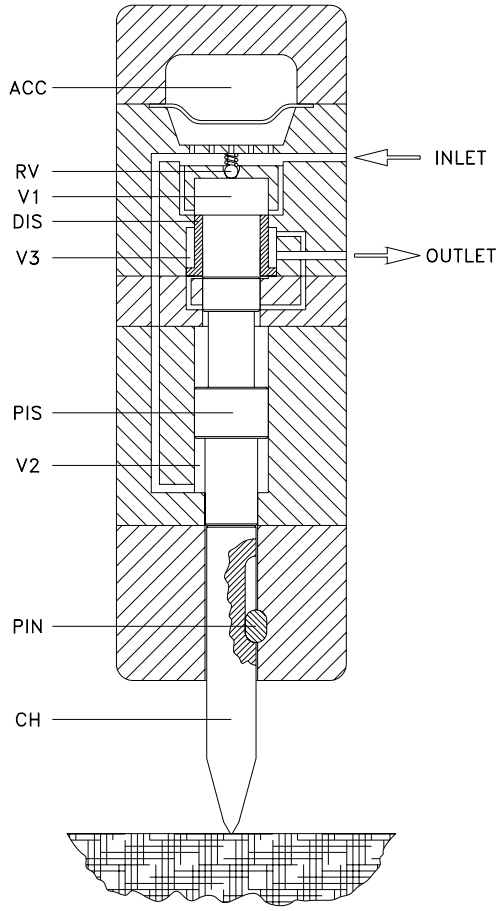

Fig. 1: *Schematic drawing of a hydraulic breaker (adapted from European Patent no. 0426928)*

Thus, referring to Fig. 1 where the distributor is in its idle position, the downward push chamber is connected to the high pressure circuit and the distributor can start its upward stroke. At first it closes the communication between downward push chamber and high pressure circuit, then it opens the communications between the same chamber and the low pressure circuit. The chamber suddenly depletes so high pressure constantly acting on the upward push chamber (V2) causes the piston to leave its bottom dead center. One can easily realize that there is a considerable difference in upward and downward push areas. As a matter of fact, the surface receiving the working push is larger, e.g. in a ratio equal to four as in the breaker considered in this work, than the piston ring surface on which high pressure is always exerted (volume V2). When the piston goes beyond the current distributor position, fluid in the downward push chamber results trapped. The relief valve (RV), present in this chamber, should prevent pressure from overshooting certain limits, so it acts as anti-shock valve. Now the piston keeps on climbing whereas the distributor begins to move downward, since the fluid at its bottom communicates with the low pressure circuit. When the downward distributor opens the communication between downward push chamber and high pressure circuit, the start of percussion occurs. The piston has reached its top dead center and its velocity instantaneously changes, becomes negative and increases progressively till the piston strikes the chisel. From the start of percussion up to the impact against the chisel, the motion of the piston results almost uniformly accelerated and the downward push chamber is fed not only by the pump but also by fluid leaving the upward push chamber and by the previously charged accumulator which is now depressurizing. When the downward piston, before reaching its bottom dead center, allows high pressure fluid to push the bottom of the distributor, which was occupying its idle position, another cycle can take place.

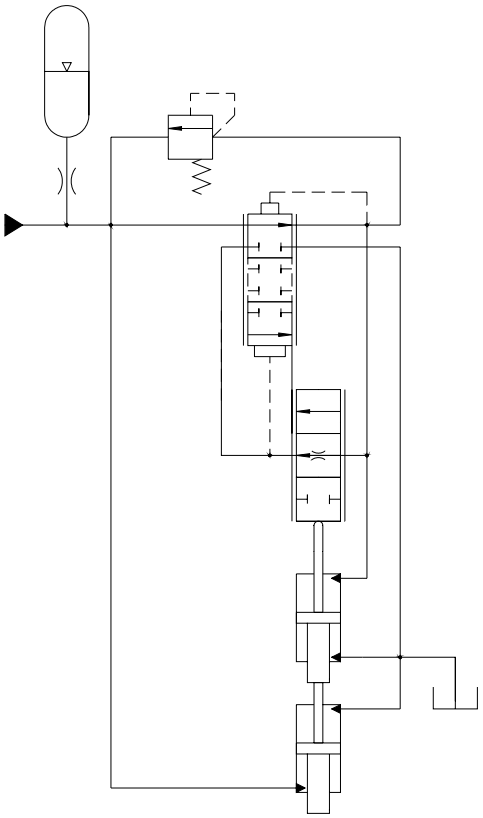

Fig. 2: *Breaker equivalent hydraulic circuit*

Figure 2 represents the translation of the working principle of the breaker into the standard symbols and proposes its equivalent hydraulic circuit. All the previously discussed elements are here reported, with reference to the accumulator, the relief valve, the distributor represented by means of a continuous positioning valve, intercepting first the high pressure fluid, and to the striking piston. Particular attention should be paid to the valve drawn at the middle of the circuit representing the variable orifice between the bottom of the distributor and the top of the piston and clearly dependent on their relative displacements. As it will be better highlighted later, it realizes a sort of timing of the dynamics of the distributor with respect to the piston one.

1.3 Research objectives

As far as this work is concerned, a model of the breaker is a preliminary step to get information about its working principle. This paper aims at simulating the hydraulic circuit of the breaker with reference to the real geometry of a commercial one, taking into account the real dimensions of the parts, the clearances, the bodies masses in order to develop a reliable model. In the next sections, brief descriptions of the model and of a first experimental activity will follow, then main results of the model will be presented and discussed.

2 Working Behaviour Model

To study the performance of the breaker, a specific model was developed. Governing equations were solved in the AMESim™ environment, where proper equations were added and implemented by the authors in order to tune the overall model. Once the breaker geometry has been fixed, the model input essentially consists of the flow rate supplied by the positive displacement pump of the hydraulic circuit. The main outputs are pressure evolutions in all the chambers, volumetric flow rates and dynamics of the moving elements as well. Figure 3 shows the lay-out of the model developed in the simulation environment. Some submodels and routines were written in C language and AMESet™ to manage flow passage areas characterized by particular geometry.

In the next two paragraphs, the basic formulations of the most important phenomena of the physical system will be reported, referring to more exhaustive documents (Imagine SA, 2004) as for the modelling details characteristic of the simulation environment.

2.1 Mechanical model

Newton's law was used to model the movements of both distributor and piston.

However, in such a hydraulic appliance, the main forces acting on the two masses simply consist of pressure forces and mass to mass interactions (impact forces). Thus, as regards the piston, it is possible to write:

$$m_p \cdot a_p = \sum F_p \tag{1}$$

Gravimetric force, even if taken into account, is negligible if compared to hydraulic forces. Thus, the standard model of a simple forced harmonic oscillator with mass, spring and damper here is not necessary. However, a certain viscous damping is always present. As a matter of fact, a fixed clearance, here modelled neglecting any possible eccentricities or misalignments, causes damping forces modelled according to

$$F_d = \mu \cdot \frac{\pi \cdot D_{p1} \cdot L_{sp}}{\delta} \cdot v_p \tag{2}$$

with reference to the geometry schematically shown in Fig. 4.

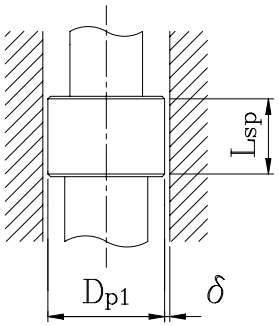

Fig. 4: *Schematic drawing of the central body of the piston*

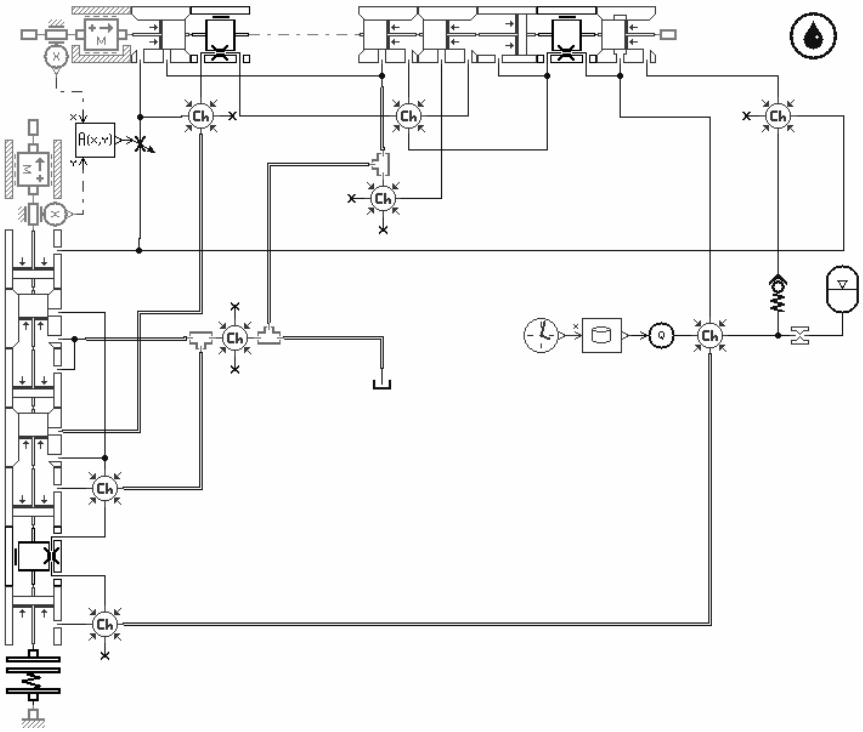

Fig. 3: *Lay-out of the model developed in the AMESim™ environment*

Every moving element was schematised according to only one mass since axial deformations due to high pressure are negligible if compared to the actual length and stroke. As for mass to mass interactions, impact is considered and modelled only when the piston strikes the chisel, as schematized in Fig. 5.

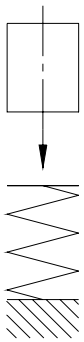

Fig. 5: *Representation of the piston striking the spring-modelled chisel*

The chisel is supposed to behave like a spring, whereas the anvil below is supposed to be infinitely stiff. Actually, such an hypothesis is justified since during the experimental campaign the anvil below the chisel consisted of a steel block whose stiffness was sufficiently larger than the chisel one. Moreover, as it will be pointed out later, the chisel equipping the tested breaker consisted of a blunt tool whose shape has a feeble penetrating rate with respect to the steel anvil. The stiffness of the chisel is here evaluated according to its geometry:

$$k_{ch} = \frac{E \cdot A_{ch}}{L_{ch}} \tag{3}$$

Thus, if x_{p0} is the elastic lower end stop of the piston (bottom dead center), the impact force is evaluated as

$$F_{ch} = k_{ch} \cdot \left(x_{p0} - x_p \right) \tag{4}$$

only if $x_p \le x_{p0}$, otherwise the piston is necessarily far from the top of the chisel and no impact force is to be taken into account when solving Eq. 1. Here it is noteworthy to underline that Eq. 4 was considered in the dynamic model of the piston only. In the current stage of modelling the lower end stop of the distributor was supposed to be ideal, then no contact force was accounted for when such a mass gets down and reaches its bottom dead center.

2.2 Hydraulic model

This model consists of several stages with particular reference to flow rates through the various opening and closing passage areas, to pressures evolution in variable or fixed volume chambers and to wave propagation phenomena in pipes connecting two chambers.

Flow rate for turbulent flow through a generic orifice was calculated using the following standard equation

$$Q = C_d \cdot A \cdot \sqrt{\frac{2}{\rho} \cdot \Delta p} \tag{5}$$

which relates the flow rate to the pressure drop across the orifice. C_d is the discharge coefficient, typically dependent on the Reynolds number, but almost constant for fully developed turbulent flow. Eq. 5 also needs the fluid density and the flow passage area. In a hydraulic breaker flow passage areas are usually variable and depend on the relative positions of the moving masses with respect to circular holes or to cylinder lateral surface shaped ports. Thus, if A is a generic function of the relative position of a moving mass, with reference to the real geometry of the machine, it is possible to refer to geometries relatively simply to model.

When the distributor leaves its bottom dead center, progressively it closes the communication between the supply line and the downward push chamber at the top of the piston. Then, considering that the circular edge of the distributor presents a negative overlap with reference to the high pressure communication consisting of a cylinder lateral surface shaped port, the area A_1 may be simply calculated as

$$A_1(x_d) = \pi \cdot D_{d1} \cdot (b_{hp} - x_d) \tag{6}$$

with reference to the geometry schematically shown in Fig. 6. Such a passage area exists if the distributor displacement does not exceed b_{hp}, otherwise high pressure fluid cannot enter the downward push chamber.

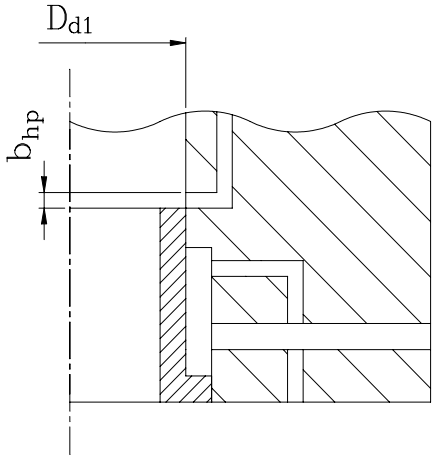

Fig. 6: *Schematic drawing of the distributor ready to leave its bottom dead center*

Focusing attention on the bottom of the distributor, and referring to the drawing shown in Fig. 1, communication with the low pressure line is possible by means of circular holes. Then passage area consists of circular segments. It is the common case of a spool valve moving over a circular hole (Nervegna, 1998; Walters, 1991), schematically shown in Fig. 7.

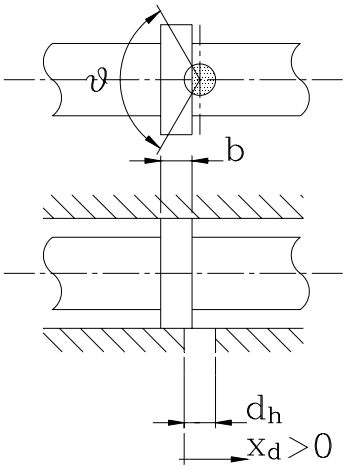

Fig. 7: *Spool valve moving over a circular hole*

With reference to Fig. 7 and considering n_h holes, in order to evaluate the passage area for the flow rate to the low pressure line from the annular volume between the distributor and the casing (V3 in Fig. 1), use of the following equation was made:

$$A_2(x_d) = n_h \cdot \left\{ \frac{\pi}{4} \cdot d_h^2 - \left[\frac{d_h^2}{4} \cdot \arccos\left(1 - \frac{2 \cdot x_d}{d_h}\right) - \right.\right. \\ \left.\left. + \frac{d_h^2}{8} \cdot \sin\left(2 \cdot \arccos\left(1 - \frac{2 \cdot x_d}{d_h}\right)\right) \right] \right\} \quad (7)$$

From Fig. 1 and 6, it is possible to realize that when the distributor goes beyond a fixed position, the downward push chamber at the top of the piston, full of high pressure fluid just an instant before, may deplete since there will be flow rate from this chamber to the tank. Such an event allows the piston to move from its bottom dead center toward a top dead center generally dependent on the nature of the material to crumble (European Patent no. 0426928). The flow rate causing the depletion of the downward push chamber depends on a passage area which consists again of circular segments, like the area A_2. Thus, a new area may be evaluated in a way similar to the one used to write Eq. 7:

$$A_3(x_d) = n_h \cdot \left\{ \frac{d_h^2}{4} \cdot \arccos\left(1 - \frac{2 \cdot x_d}{d_h}\right) - \right. \\ \left. + \frac{d_h^2}{8} \cdot \sin\left(2 \cdot \arccos\left(1 - \frac{2 \cdot x_d}{d_h}\right)\right) \right\} \quad (8)$$

Contrary to what Eq. 7 formulates, Eq. 8 represents a passage area increasing with the position of the distributor. The two last equations were formulated with reference to Fig. 7, for the sake of simplicity, where the spool movement is assumed to be positive when starting from a negative overlap equal to d_h.

Figure 8 shows these passage areas uncovered by the edge of the spool valve. Areas and displacements were normalized with respect to the hole areas and diameter respectively.

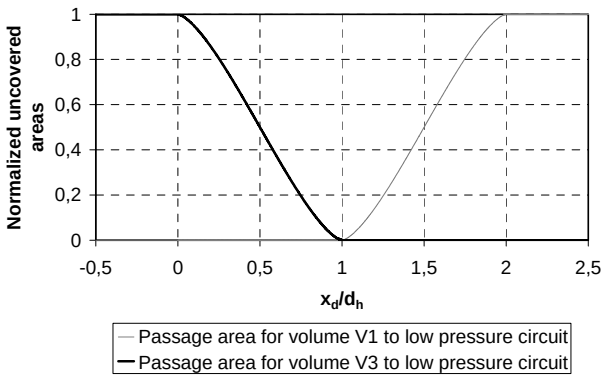

Fig. 8: *Normalized passage areas uncovered by a spool passing through a hole*

Figure 8 was drawn fixing the height of the flange (*b*) equal to the hole diameter d_h. In the real geometry of the machine, the overlap is larger, as one can notice from Fig. 1. However, passage areas reported in Fig. 8 do not change but they simply shift to the right.

When the distributor closes the communication between volume V3 and low pressure circuit (the passage area may be evaluated by means of an equation similar to Eq. 7), its movement is suddenly stopped by a hydraulic cushion, as shown in Fig. 9. As a matter of fact, beyond this value the fluid in volume V3, at its minimum value, results trapped and acts as a hydraulic shock absorber.

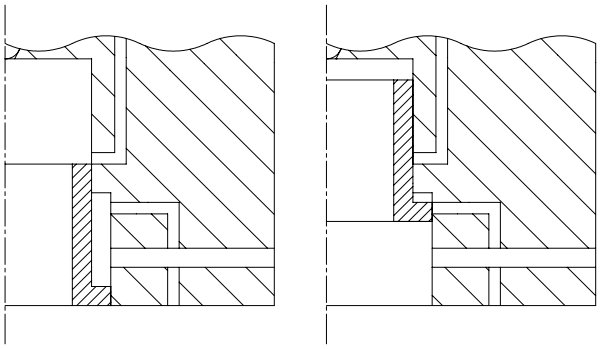

Fig. 9: *Distributor at its bottom dead center (on the left) and at its hydraulic end stop (on the right)*

As for the piston, when it moves upward and is going to enter the distributor, the minimum passage area governing the flow rate from volume V1 towards the low pressure line moves from A_3 to the area realizing between the bottom of the distributor and the top of the piston itself. With reference to the simple geometry shown in Fig. 1, evaluating such a new area leads to a formulation similar to the one proposed in Eq. 6, where the passage area varies with linearity, depending on the relative position between distributor and piston. Actually, the real geometry is somewhat complicated and the formulation is here omitted for the sake of brevity.

Correctly modelling flow rates entering and exiting a generic lumped volume needs to take volumetric losses into account. Thus, a reliable model should predict leakage phenomena due to manufacturing tolerances as accurately as feasible. In real displacement machines (Ivantysyn and Ivantysynova, 2002), lubrica-

tion gaps between the sliding surfaces exist and deformations of the machine parts occur because of the elasticity of the material with pressure and temperature. Of course, these gaps are necessary, as design requirements, when the parts have relative motions to each other. Till these gaps perform a sealing function, i.e., the separation of volumes at different pressures, fluid flows through the gap due to the pressure difference.

Volumetric losses were modelled as two dimensional, laminar and incompressible flow, according to the common formulation of Poiseuille flow. With reference to Fig. 4, leakage flow rate was evaluated according to

$$Q_{\text{loss},1} = \frac{\pi \cdot D_{\text{p1}} \cdot \delta^3}{12 \cdot \mu \cdot L_{\text{sp}}} \cdot \Delta p \tag{9}$$

On the other hand, an entrained flow, due to the viscosity of the fluid which adheres to the moving masses, cannot be neglected. As a matter of fact, a Couette flow occurs owing to the adhesion of fluid particles on the moving surfaces. Always referring to Fig. 4, the above mentioned flow was modelled as:

$$Q_{\text{loss},2} = \frac{\pi}{4} \cdot \left[\left(D_{\text{p1}} + 2 \cdot \delta \right)^2 - D_{\text{p1}}^2 \right] \cdot \frac{v_{\text{p}}}{2} \tag{10}$$

where the piston moves with respect to a fixed reference. In several cases, both gap (Couette and Poiseuille) flows superimpose. Basically, the number, the geometry and the dimensions of the sealing gaps depend on the type and design features of the displacement machine, which influence the values of the volumetric losses significantly.

Pressure level inside variable or fixed volume chambers should be accurately evaluated since hydraulic forces are the main causes for the movement of both distributor and piston. Pressures in each chamber were evaluated on the basis of the basic equation:

$$\frac{dp_{\text{i}}}{dt} = \frac{\beta}{V_{\text{i}}} \cdot \left(\sum Q_{\text{i}} - \frac{dV_{\text{i}}}{dt} \right) \tag{11}$$

where the *i*-th chamber volume variation and the sum of all the entering and exiting volumetric flow rates are taken into account. Of course, the volume variation term is dependent on the relative position of distributor and piston.

Wave propagation phenomena in a pipe connecting two chambers are considered and modelled. A state variable representing the pressure at the mid point of the pipe is introduced:

$$\frac{\partial p}{\partial t} = -\frac{\beta}{\Omega} \cdot \frac{\partial Q}{\partial x} \tag{12}$$

The compressibility of the fluid is taken into account by using an effective bulk modulus (Imagine SA, 2000). Pipe friction is accounted for by using a factor depending on the Reynolds number and the relative roughness. The inertia of the fluid is also considered by a flow rate state variable at each end of the pipe. The derivatives of the flow rate at the two ends are calculated using the following equation

$$\frac{\partial Q}{\partial t} = \frac{\Omega}{\rho} \cdot \frac{\partial p}{\partial x} - v \cdot \frac{\partial Q}{\partial x} - \frac{\lambda \cdot Q^2 \cdot sign(Q)}{2 \cdot d \cdot \Omega} \tag{13}$$

The model simulating the hydraulic pipes is a complex distributed parameter, suitable for situations where wave dynamics is likely to be important (Imagine SA, 2004). The submodel has two external state variables representing the flow rates at each end of the line, together with six internal pressure state variables and five internal flow rate state variables. Moreover, the simulation environment models friction as frequency dependent by means of a utility function, so that the flow rate derivative is modified to include frequency dependent friction. The phenomena under study, characterized by pulses with high frequencies, suggested this choice.

These last two equations were just used with reference to the pipes connecting the inlet of the breaker to the upward push chamber (V2). As regards the other shorter lines, the use of a simpler submodel was made, where friction depends no more on frequency and no internal pressure state variable is accounted for.

As for the nitrogen gas in the accumulator, it is assumed to obey a polytropic gas law of the form:

$$p \cdot V^{\gamma} = const \tag{14}$$

where the constant is defined by the precharge pressure and the accumulator volume. The hydraulic fluid within the accumulator was assumed to have the same pressure as the gas. In order to prevent problems that would occur if the gas volume tended to zero, when it becomes 1/1000 of the nominal accumulator volume, the accumulator is assumed to be fully charged. In order to simulate pressurization and depressurization stages of the accumulator, use of the following equation was made

$$\frac{dp_{\text{gas}}}{dt} = \frac{\gamma \cdot p_{\text{gas}}}{V_{\text{gas}}} \cdot Q_{\text{acc}} \tag{15}$$

The two stages depend on the sign of Q_{acc}, positive or negative if entering or exiting respectively.

Lastly, the management of the fluid properties such as bulk modulus and density was remitted to the simulation tool. Reference to (Imagine SA, 2000) may inform about the fluid model.

3 Experimental Campaign

It is ascertained that in a hydraulic breaker fluid power turns into the reciprocating motion of the piston, accelerated with high velocity to strike the top of the chisel. The kinetic energy of the piston during its impact against the chisel turns into a deformation wave, propagating inside the chisel itself. Afterwards, the wave moves from the top of the chisel towards the material to crumble. The energy conveyed by the piston consists of its kinetic energy at the instant of the impact:

$$E_{\text{k}} = \frac{1}{2} \cdot m_{\text{p}} \cdot v_{\text{p,i}}^2 \tag{16}$$

This energy is transferred to the chisel and is completely present in the first deformation wave, which should be measured to evaluate the blow energy of the breaker. However, such an energy is lower than the kinetic energy of the piston, owing to unavoidable

transmission losses. In order to take this energy transmission by the piston, a specific testing procedure consisting of the CIMA measuring guide for tool energy rating (www.aem.org), with reference to tests and data elaboration, suggests to measure the deformation of the chisel itself by means of strain gages mounted on the chisel of the breaker. Together with such a deformation, the procedure demands the measurement of the oil inlet and outlet pressures, of the flow rate supplied by the pump and of the oil temperature, with proper transducers. Here, these measurements, with direct reference to oil inlet pressure and flow rate, were used to try to verify the theoretical results advanced with the current test case. Figure 10 shows a schematic diagram of the experimental hydraulic system with its main components. The breaker was essentially fed by a variable displacement pump driven by an electric motor with maximum power up to 25 kW. The viscosity of the working fluid was kept constant by maintaining constant oil temperature. The adopted instrumentation consisted of a flowmeter of the Parker SCQ150 type and a pressure sensor of the Parker SCPT600 type. Both hydraulic signals were simultaneously digitised using an analogic/digital acquisition board (National Instrument AT-MIO-16E-10) on a PC. Data acquisition and their next elaboration were carried out in the LabVIEW™ environment.

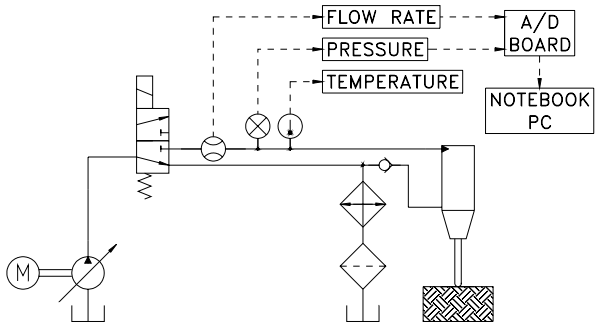

Fig. 10: *Schematic diagram of the experimental system*

As for the tool equipping the breaker, it was not a standard chisel, but, as previously mentioned, a blunt tool, clearly characterized by feeble penetrating rate with respect to the steel anvil, more rigid than the tool itself. This tool was just adopted in order to keep it from considerably penetrating the anvil. As a matter of fact, if the tool penetrates the anvil, its progressive breaking will cause the breaker body to follow the tool in its downward penetrating motion, owing to its weight and to the pin necessary to fix the tool to the breaker casing (Fig. 1). Such considerations would justify the development of the current model, where the motion of the breaker casing was neglected.

The next Fig. 11 shows accumulator pressure and volumetric flow rate entering the breaker. Pressure and flow rate are periodical and strictly correlated. The former is characterized by a saw toothed shape and when it suddenly decreases, this event is accomplished with a considerable increase in flow rate. Such a phenomenon may be explained considering that when the pressure quickly decreases, the piston is moving downward to strike the chisel. During this period high pressure oil is directed to the inlet of the breaker from the upward push volume and from the accumulator, where a depressurization occurs, so flow rate increases. Oscillation phenomena are related to the functioning principles of the breaker and to the dynamic pressure waves propagating inside the breaker itself. As a matter of fact, the downward movement of the piston generates very quick depressurizations inside the accumulator and the following rebound of the piston causes oil hammer phenomena characterized by pressure overshooting up to 40 MPa in the downward push chamber, according to the results of the model presented in the next section.

4 Simulation Results

First of all, it is to be underlined that all the theoretical results presented in this section were obtained feeding the breaker with the measured inlet flow rate, according to its waveform presented in Fig. 11. As a matter of fact, it represents the real input to the breaker.

As for the experimental data, the possible comparison with theoretical results actually concerns only the pressure variation inside the accumulator. At the current stage of this research activity there are no real data referring to the movements of the masses inside the breaker, even granting the actual capability in such measurements. Thus, the only comparison between theoretical and experimental accumulator pressures is here reported and shown in Fig. 11, as preliminary validation of the actual model.

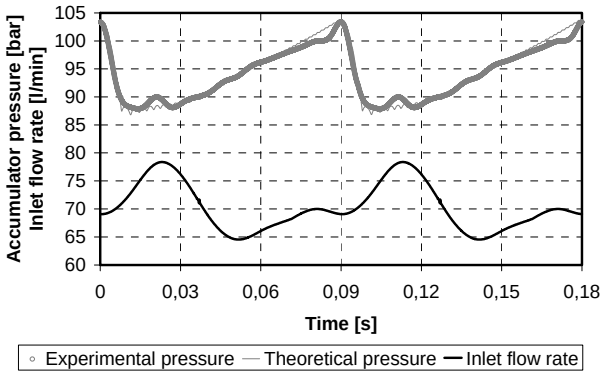

Fig. 11: *Comparison between experimental and theoretical accumulator pressures and experimental inlet flow rate*

The real evolution seems to be sufficiently reproduced, especially with reference to the saw toothed shape. As regards the working period, it is equal to the experimental one (90 ms). Of course, such a remark was desirable even if trivial.

In order to have only one value referring to the inlet pressure, the averages of the experimental and theoretical signals were calculated according to the following formulation

$$p_{acc,m} = \frac{1}{T} \cdot \int_T p_{acc} \cdot dt \qquad (17)$$

Two values equal to 94 and 94.2 bar, as for the experimental and theoretical pressures respectively, were calculated. When these values are multiplied for the mean flow rate supplied by the pump of the hydraulic circuit, it is possible to get information about the input power P_p to the breaker. These calculations may be useful in order to evaluate the efficiency of the machine. Thus, considering the mean inlet flow rate (70 l/min), the input power P_p results equal to 10.97 kW.

The comparison shown in Fig. 11 encourages to present other results, referring to the dynamics of both distributor and piston. Figure 12 shows the displacements of these theoretical moving elements in the same time window of Fig. 11.

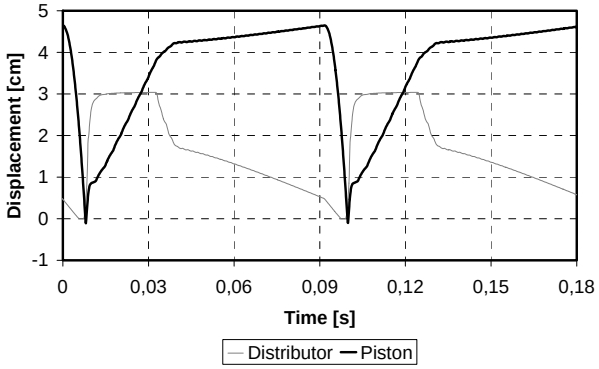

Fig. 12: *Theoretical displacements of distributor and piston*

It is possible to appreciate that when the downward distributor opens the communication between high pressure circuit and downward push chamber ($x_d \leq 5$ mm), the piston has reached its top dead center and the start of percussion begins from this position. Later the piston moves downward, crosses a certain position and allows high pressure fluid to act at the bottom of the distributor.

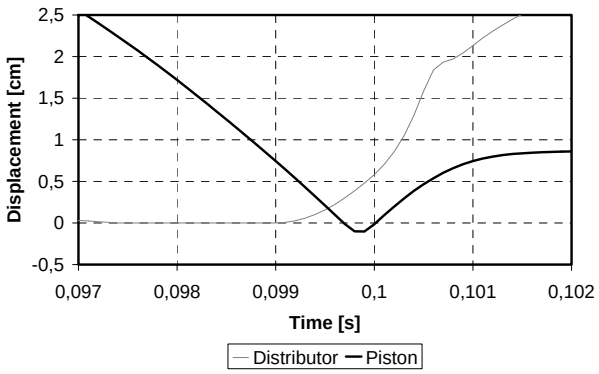

Fig. 13: *Timing allowing the distributor to leave its seat before the impact between piston and chisel*

Such a situation is better represented in Fig. 13 where an enlargement of Fig. 12 is shown and one can clearly realize about this sort of timing previously mentioned and represented by means of the continuous positioning valve at the middle of the equivalent hydraulic circuit reported in Fig. 2. Now the distributor starts to move upward, whereas the piston keeps on falling down till it strikes the chisel. At the instant of the impact, the piston, after having crushed the top of the chisel ($x_p < 0$), bounces and the intensity of such an event depends on the material to crumble (European Patent no. 0426928). Owing to a considerable rebound, the volume at the top of the piston, which is trapped since the distributor has already closed any connection, is subject to a very rapid pressure increase, allowing the distributor to reach its higher position. Now, the volume where pressure has overshot just an instant before may deplete because of the open communication to the low pressure circuit. At the two extremities of the piston two different pressures act then its movement is possible even if it moves slowly if compared to the downward stroke. When the piston reaches and overtakes the distributor, the downward push volume is trapped again and the distributor begins to move downward since the fluid at its bottom communicates with the low pressure circuit. Meanwhile, the piston keeps on climbing even if a considerable change in its velocity has occurred. Then, the downward distributor opens the communication between downward push volume and high pressure circuit and another cycle takes place (Fig. 12).

As for the velocities of the two masses, Fig. 14 shows the results of the model. Here attention should be paid to the velocity of the piston just before the impact against the chisel. The theoretical value is equal to 11.15 m/s.

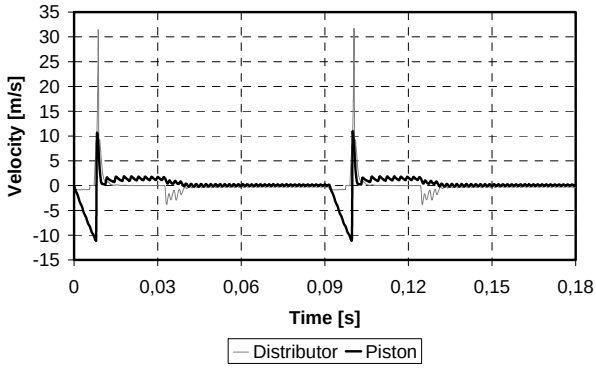

Fig. 14: *Theoretical velocities of distributor and piston*

Thus, considering Eq. 16 (the mass of the piston is equal to 10.5 kg) and the working frequency as well, it is possible to evaluate the power transmission as

$$P_T = E_k \cdot f \tag{18}$$

Energetic considerations lead to an efficiency expressed by the ratio between the power transmitted to the chisel and the input power:

$$\eta = \frac{P_T}{P_p} = 0.66 \tag{19}$$

The previous value should not strictly represent the global efficiency, since mechanical transmission losses may occur when the blow energy moves from the impacted extremity of the chisel towards the material to crumble. Thus, the real efficiency should be a bit lower. Of course, higher values of efficiency may be achieved with an optimized design of the hydraulic machine. However, it is to be underlined that part of the hydraulic power supplied by the pump of the hydraulic circuit

to the breaker is inevitably thrown away to move the distributor. Moreover, leakage flow rates represent another source of loss and the actual fluid is compressible. At least three causes of energy losses are just mentioned to justify the value returned in Eq. 19.

Another noteworthy result suggested by the model concerns the pressure evolution inside the downward push chamber (V1 in Fig. 1). Fig. 15 shows this pressure together with the accumulator pressure. For the sake of greater clearness, the window was cut on its upper part, even if pressure overshoots up to 400 bar.

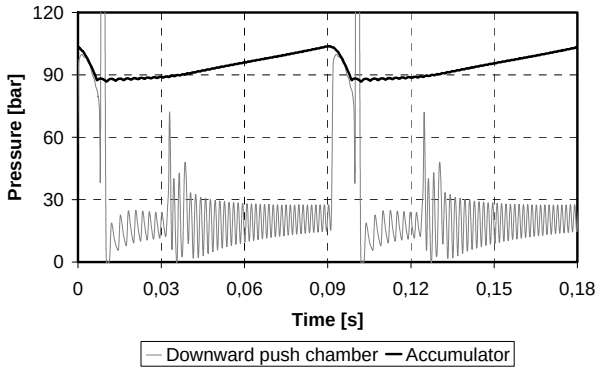

Fig. 15: *Theoretical pressures inside the downward push chamber and the accumulator*

Pressures evolutions reported in Fig. 15 are considered to be particularly interesting since the two pressure levels are direct responsible for the piston movement, then for energy transmission to the chisel. As a matter of fact, the accumulator pressure constantly acts on the upward push chamber (V2), in spite of waves propagation inside the pipes connecting the chamber itself and the accumulator, or rather the breaker inlet. From Fig. 15 it is possible to appreciate that the pressure inside the downward push chamber is lower than the accumulator pressure for a considerable time interval. Moreover, as for this time interval, simulation suggested that pressure in the downward push chamber (V1) is characterized by high frequency oscillations, as long as the chamber itself results trapped. Such oscillations should be caused by pressure waves in the pipes connecting the inlet of the breaker with the upward push chamber (V2), reflecting on the piston acceleration, then on pressure inside the downward push chamber. The latter is almost equal to the accumulator pressure, following its shape, once the downward distributor opens the communication with the high pressure circuit and the start of percussion occurs. Of course, from this instant pressure levels in both accumulator and downward push chamber decrease since a large amount of fluid is required to fill this chamber, which has a strongly positive volume variation. However, when the piston has reached its bottom dead centre and struck the chisel, its rebound causes a very quick pressure rise, which may find vent directly to the inlet of the breaker, thanks to the anti-shock valve (RV) intuitively put inside the downward push chamber, as shown in Fig. 1.

One could object that the results proposed in the previous figures depend on the particular waveform characteristic of the inlet flow rate, since all the presented theoretical results come from such a flow rate. In order to meet this right objection, another simulation was run replacing the actual inlet flow rate with its mean value. As unexpected result, no considerable variations with respect to the previous results appeared. The only exception consisted of a longer working period, increasing from 90 ms to 92 ms, leading to a relative error equal to 2.2%. This is a very remarkable result since, when running a simulation, fixing constant inlet flow rate is an obliged choice. Flow rate oscillations and period are unknown a priori. Moreover, fixing different constant values of inlet flow rate allows to better understand the hydraulic behaviour of the breaker, with particular reference to working pressure, frequency and piston velocity at the instant of the impact.

5 Conclusion

This case study dealt with the simulation of the working behaviour of a hydraulic breaker. The objective was to build a very detailed parameterized model that would allow the reproduction of physical phenomena and measurement results. Experimental data were used to verify the model predictions, with reference to the accumulator pressure. An appreciable agreement between experimental and theoretical pressure and frequency encouraged about the quality of the model, so the dynamic behaviour of the moving masses was presented and discussed.

Once certain physical behaviours have been fully understood, the current model may be used to test and validate several design solutions and to provide valuable help to propose some innovating solutions for the optimisation of at least the hydraulic system of the breaker, being the breaker itself a complex multi-body mechanical system.

Thus, the current work represents the first step towards further theoretical and experimental research. The theoretical research will be oriented to a more complex model eventually taking into account possible movements or vibrations of the breaker casing, influencing the hydraulic system of the machine. The experimental research will be carried out in order to equip the breaker with all those measurement instruments allowing for a better and exact validation of the simulation model.

6 Acknowledgements

The authors gratefully acknowledge Imagine SA for the use of the AMESim™ software and eng. Antonio Andriani of Tecna (Acquaviva delle Fonti, BA, Italy) for the experimental support.

Nomenclature

A, A_k	Flow passage areas (k = 1…3)	[m^2]
A_{ch}	Chisel cross sectional area	[m^2]
C_d	Discharge coefficient	[-]
d	Pipe diameter	[m]
E	Young's modulus of elasticity	[Pa]
E_K	Kinetic energy of the piston at the instant of the impact against the chisel	[J]
f	Working frequency	[s^{-1}]
F_d	Damping force	[N]
F_p	Generic force acting on the piston	[N]
k_{ch}	Chisel stiffness	[$N \cdot m^{-1}$]
L_{ch}	Chisel length	[m]
m_d, m_p	Distributor and piston masses	[kg]
p_i	Pressure level inside the i-th chamber	[Pa]
$p_{acc,m}$	Accumulator mean pressure level	[Pa]
P_P	Power supplied by the pump	[W]
P_T	Power transmitted to the chisel	[W]
Q	Volumetric flow rate	[$m^3 \cdot s^{-1}$]
Q_{acc}	Volumetric flow rate entering or exiting the accumulator	[$m^3 \cdot s^{-1}$]
Q_i	Volumetric flow rate entering or exiting the i-th chamber	[$m^3 \cdot s^{-1}$]
T	Working period	[s]
v	Fluid velocity	[$m \cdot s^{-1}$]
$v_{p,i}$	Piston velocity at the instant of the impact against the chisel	[$m \cdot s^{-1}$]
V_i	Volume of the i-th chamber	[m^3]
x_d, x_p	Distributor and piston displacements	[m]
v_d, v_p	Distributor and piston velocities	[$m \cdot s^{-1}$]
a_d, a_p	Distributor and piston accelerations	[$m \cdot s^{-2}$]
Δp	Pressure drop	[Pa]
Ω	Inner cross sectional area of a pipe	[m^2]
β	Fluid bulk modulus	[Pa]
δ	Radial gap	[m]
γ	Polytropic index	[-]
η	Efficiency in power transmission	[-]
λ	Friction factor	[-]
μ	Fluid dynamic viscosity	[Pa·s]
ρ	Fluid density	[$kg \cdot m^{-3}$]

References

Gorodilov, L. V. 2000. Analysis of Working Cycle of Hydraulic Impact Machine Using Similarity Criteria. *Journal of Mining Science*, Vol. 36, no. 5, pp. 476-480.

Gorodilov, L. V. 2002. Investigation into Characteristics of Working Cycles of Hydraulic Percussive Machines with Ideal Distributor. *Journal of Mining Science*, Vol. 38, no. 1, pp. 74-79.

Ivantysyn, J. and **Ivantysynova, M.** 2000. *Hydrostatic Pumps and Motors.* Academia Books International, New Delhi.

Imagine SA. 2004. AMESim™ version 4.2 electronic manual.

Imagine SA. 2004. AMESet™ version 4.2 electronic manual.

Imagine SA. 2002. AMESim™ Standard Fluid Properties, Technical Bulletin no. 117.

Nervegna, N. 1998. *Directional, Pressure and Flow Control Valves*, Politeko, Turin (in Italian).

Vitulano, M. 1968. *Directional control valve to obtain in a hydraulic appliance the alternative motion of a piston operatingto charge and fire a tool, specially suitable for hydraulic hammers*. European Patent no. 0085279, 09.07.1986.

Vitulano, M. 1991. *Method to automatically adjust the functional parameters of a percussion apparatures*. European Patent no. 0426928, 15.05.1991.

Walters, R. B. 1991. *Hydraulic and electro-hydraulic control systems*, Elsevier Science Publishers.

Association of Equipment Manufacturers. *CIMA Pamphlet Explains Tool Energy Rating*. Avaiable from: http://www.aem.org/News/AEMNews/Details.asp?P=105 [Acessed 24 June 2005].

Antonio Giuffrida
Born on April 5th 1974 in Catania, Italy. He received his MSc. Degree in Mechanical Engineering in 1999 from University of Catania and PhD. Degree in Energy Systems and Environment from University of Lecce, Italy. From 1998 to 1999 he spent a training period in Polytechnic of Turin under supervision of professor N. Nervegna (Fluid Power Group). He is very active in modelling, simulation and testing of fluid power components.

Domenico Laforgia
Full Professor of Energy Systems and Environment at the University of Lecce, Italy and Dean of the Engineering Faculty. Director of the Research Center on Energy and Environment. Founder and senior partner at STIM Engineering Ldt. a professional corporation that boasts a wide range of skills including: consulting, engineering, and training services in the following fields of activity: industrial design, energy, ecology and environment, industrial property, technological innovation. Visiting fellow at the Mechanical and Aerospace Department at Princeton University, USA. He collaborated with ELASIS, FIAT Research Center in Southern Italy, in the development of a highly innovative Diesel injection system, known today as Common Rail and manufactured by Bosch. His work is mainly on combustion of internal combustion engines and Diesel injection systems.